ELSEVIER

Mechanisms of Development 95 (2000) 35–46

www.elsevier.com/locate/modo

The mouse rib-vertebrae mutation disrupts anterior-posterior somite patterning and genetically interacts with a *Delta1* null allele

Johannes Beckers[1], Nicole Schlautmann[2], Achim Gossler[2,*]

The Jackson Laboratory, Bar Harbor, ME 04609, USA

Received 24 February 2000; received in revised form 22 March 2000; accepted 23 March 2000

Abstract

Rib-vertebrae (*rv*) is an autosomal recessive mutation in mouse that affects the morphogenesis of the vertebral column. Axial skeleton defects vary along the anterior-posterior body axis, and include split vertebrae and neural arches, and fusions of adjacent segments. Here, we show that defective somite patterning underlies the vertebral malformations and altered Notch signaling may contribute to the phenotype. Somites in affected regions are irregular in size and shape, epithelial morphology is disrupted, and anterior-posterior somite patterning is abnormal, reminiscent of somite defects obtained in loss-of-function alleles of Notch signaling pathway components. Expression of *Dll1*, *Dll3*, *Lfng* and Notch1 is altered in *rv* mutant embryos, and *rv* and *Dll1*^{lacZ}, a null allele of the Notch ligand Delta1, genetically interact. Mice double heterozygous for *rv* and *Dll1*^{lacZ}, show vertebral defects, and one copy of *Dll1*^{lacZ} on the homozygous *rv* background enhances the mutant phenotype and is lethal in the majority of cases. However, fine genetic mapping places *rv* into an interval on chromosome seven that does not contain a gene encoding a known component of the Notch signaling pathway.

Keywords: Rib-vertebrae; Mouse; *Delta1*; Anterior-posterior somite patterning

1. Introduction

Somitogenesis is a fundamental pattern forming process that subdivides the paraxial mesoderm along the anterior-posterior body axis into a metameric series of subunits, the somites (Christ and Ordahl, 1995; Gossler and Hrabe de Angelis, 1997). The metamerism of the somites lays the basis for the segmented arrangement of the somite-derived axial skeleton. In most vertebrate species, somites are spheres of epithelial cells that are generated during gastrulation and axis elongation in a strict anterior-posterior sequence at the cranial end of the unsegmented portion of the paraxial mesoderm. Somites are subdivided into cranial and caudal halves which differ in gene expression patterns and functional properties (Keynes and Stern, 1984; 1988). Notably, this compartmentalization is essential for the restricted migration of neural crest cells through the cranial halves of somites (Teillet et al., 1987; Norris et al., 1989; Bronner-Fraser and Stern, 1991) and for the maintenance of somite borders (Stern and Keynes, 1987; Hrabé de Angelis et al., 1997). Transplantation experiments in avian embryos and gene expression patterns indicate that a meristic pattern is already present in the mesenchymal presomitic mesoderm (Kieny et al., 1972) and that anterior-posterior segment polarity is established prior to the formation of epithelial somites (Christ et al., 1974; Menkes and Sandor, 1977). Segmentation and the generation of segment polarity appear to be intrinsic properties of the presomitic mesoderm (Bellairs, 1963; Lanot, 1971; Christ et al., 1972; Brustis and Gipoulou, 1973; Christ et al., 1974; Packard and Jacobson, 1976; Packard, 1980a,b; Sandor and Fazakas-Todea, 1980; Tam and Beddington, 1986; Palmeirim et al., 1997; Forsberg et al., 1998; McGrew et al., 1998), although the presence of surface ectoderm is apparently required for the formation of epithelial somites in vivo (Sosic et al., 1997) and in vitro (Palmeirim et al., 1997).

Recent studies in various vertebrate species have identified a number of genes with essential functions in somite formation and patterning (e.g. Burgess et al., 1995; Conlon et al., 1995; Hrabé de Angelis et al., 1997; Jen et al., 1997, 1999; Saga et al., 1997; Evrard et al., 1998; Kusumi et al., 1998; Sparrow et al., 1998; Zhang and Gridley, 1998; del Barco Barrantes et al., 1999; Takke and Campos-Ortega,

* Corresponding author. Tel.: +49-511-532-4443; fax: +49-511-532-4283.

E-mail address: gossler.achim@mh-hannover.de (A. Gossler).

[1] Current address: GSF, Institute of Experimental Genetics, Ingolstädter Landstrasse 1, 85764 Neuherberg, Germany.

[2] Current address: Institut für Molekularbiologie, MHH, 30625 Hannover, Germany.

0925-4773/00/$ - see front matter
PII: S0925-4773(00)00323-3

1999). Many of these genes encode known or putative components of the Notch signaling pathway. The Notch signaling pathway constitutes an evolutionary conserved cell-to-cell signaling mechanism that regulates cell fate decisions in diverse organisms (Artavanis-Tsakonas et al., 1995; Campos-Ortega, 1995; Artavanis-Tsakonas et al., 1999). In *Drosophila*, for example, it has important functions during neurogenesis (Campos-Ortega, 1995), in epithelial-mesenchymal transitions in derivatives of all germ layers (Hartenstein et al., 1992; Tepass and Hartenstein, 1995), and in the dorsoventral patterning of the wing imaginal disc (de Celis et al., 1996; Doherty et al., 1996). Vertebrate homologues of known components of the Notch signaling pathway are expressed in the presomitic mesoderm and/or somites in spatially restricted and dynamic patterns (Bettenhausen et al., 1995; Williams et al., 1995; Dunwoodie et al., 1997; Johnston et al., 1997; Forsberg et al., 1998; McGrew et al., 1998). Disturbance of Notch signaling in loss-of-function and gain-of-function experiments leads to severe defects in somitogenesis indicating an essential role for Notch pathway genes in defining or refining intra- and inter- somitic borders and in establishing anterior-posterior segment polarity (Hrabé de Angelis et al., 1997; Jen et al., 1997, 1999; Evrard et al., 1998; Kusumi et al., 1998; Sparrow et al., 1998; Zhang and Gridley, 1998; Takke and Campos-Ortega, 1999).

In *Drosophila* (e.g. Brand and Campos-Ortega, 1990; Xu et al., 1990; Qi et al., 1999) and *C. elegans* (e.g. Sundaram and Greenwald, 1993) mutations in different components of the Notch signaling pathway show dosage sensitive genetic interactions. Such genetic interactions have facilitated the identification of novel components of the Notch pathway and their functional analysis. Also in mice, loss-of-function alleles of the Notch ligands Delta1 (*Dll1*^{lacZ}, Hrabé de Angelis et al., 1997) and Delta3 (*Dll3*^{pu}, Kusumi et al., 1998) interact genetically (J. Beckers and A. Gossler, unpublished observation). This suggests that also in mice the analysis of genetic interactions may lead to the identification of novel components of the Notch signaling pathway relevant for somitogenesis. Towards this aim we have begun to analyze spontaneous mutations in mice affecting somite formation and patterning.

Here, we report on the phenotypic and genetic analysis of the rib-vertebrae (*rv*) mutation. Rib-vertebrae is a spontaneous, autosomal recessive mutation that causes fusions of the lower ribs and malformations of vertebrae. Defects have been histologically analyzed and traced back to somite deformities on embryonic day 12 (Theiler and Varnum, 1985). However, neither the onset and primary nature of somite defects, nor the chromosomal localization of *rv*, the affected gene, or the molecular nature of the mutation are known. Our analysis shows that already on embryonic day 9 somite defects are apparent. Similar to the loss-of-function alleles of the Notch ligands Delta1 (*Dll1*^{lacZ}, Hrabé de Angelis et al., 1997) and Delta3 (*Dll3*^{pu}, Kusumi et al., 1998), *rv* affects anterior-posterior somite polarity. In addition, segmentation appears to be delayed. *rv* genetically interacts with *Dll1*^{lacZ} such that double heterozygotes show a mild '*rv*-phenotype' with complete penetrance whereas the vast majority of homozygous *rv* mice that carry one copy of the *Dll1*^{lacZ} allele dies perinatally. Double heterozygotes between *rv* and *Dll3*^{pu} or a targeted Notch1 null-allele show no phenotype. The *rv* mutation maps to the middle of chromosome 7 into the proximity of the *Mesp1*/*Mesp2* genes, but is distinct from these genes.

2. Results

2.1. Patterning defects in rib-vertebrae mutants

The rib-vertebrae (*rv*) mutation arose in the C57BL/6 strain, and was transferred, maintained, and originally analyzed on the C57BL/6J background (Theiler and Varnum, 1985). We transferred *rv* onto a mixed genetic 129Sv^{Pas}/C57BL/6J background to improve the breeding performance and embryo yield for the analysis of the mutant phenotype. The examination of skeletal preparations of newborn and adult mutants, and the histopathological analysis of mutant embryos showed that on the mixed genetic background the overall defects were very similar to the observations on the C57BL/6J background. In brief, we consistently observed fusions of neural arches (arrowheads in Fig. 1D; bracket in Fig. 1I) and vertebral bodies as well as split vertebrae and neural arches in the cervical, lower thoracic, lumbar and upper sacral regions (small arrow in Fig. 1I and data not shown). In all mutants, neural arch fusions resulted in a contiguous bone extending from the lower thoracic (generally posterior to T7) to the upper sacral region (bracket in Fig. 1I). In this region most neural arches were open at the dorsal midline reminiscent of a spina bifida phenotype (large arrow in Fig. 1I). In addition, in all *rv* homozygous animals multiple ribs of the lower thoracic region were fused proximally (arrowheads in Fig. 1I). In the distal tail region of *rv* homozygous mutants some irregular or fused vertebral elements were always present (Fig. 4L). Distinct vertebrae with consistently normal morphology were confined to the upper thoracic (T2–T8) and the proximal tail regions.

As on the C57BL/6 background, day 11–13 mutant embryos showed irregular mesenchymal condensations, fused somites and unevenly spaced intersegmental vessels in regions that correspond to the affected portions of the vertebral column. At these stages about 60% of mutant embryos (31/50) showed protrusions containing mesenchymal tissue in the distal region of the tail (data not shown). The histopathological analysis showed that also the regular cellular organization of somitic epithelia was generally disrupted (compare insets in Fig. 1E,F). Fused and irregular somites in the prospective cervical region were present as early as on day 8.5 (Fig. 1H), suggesting that somitic defects are present from the beginning of somitogenesis. In addi-

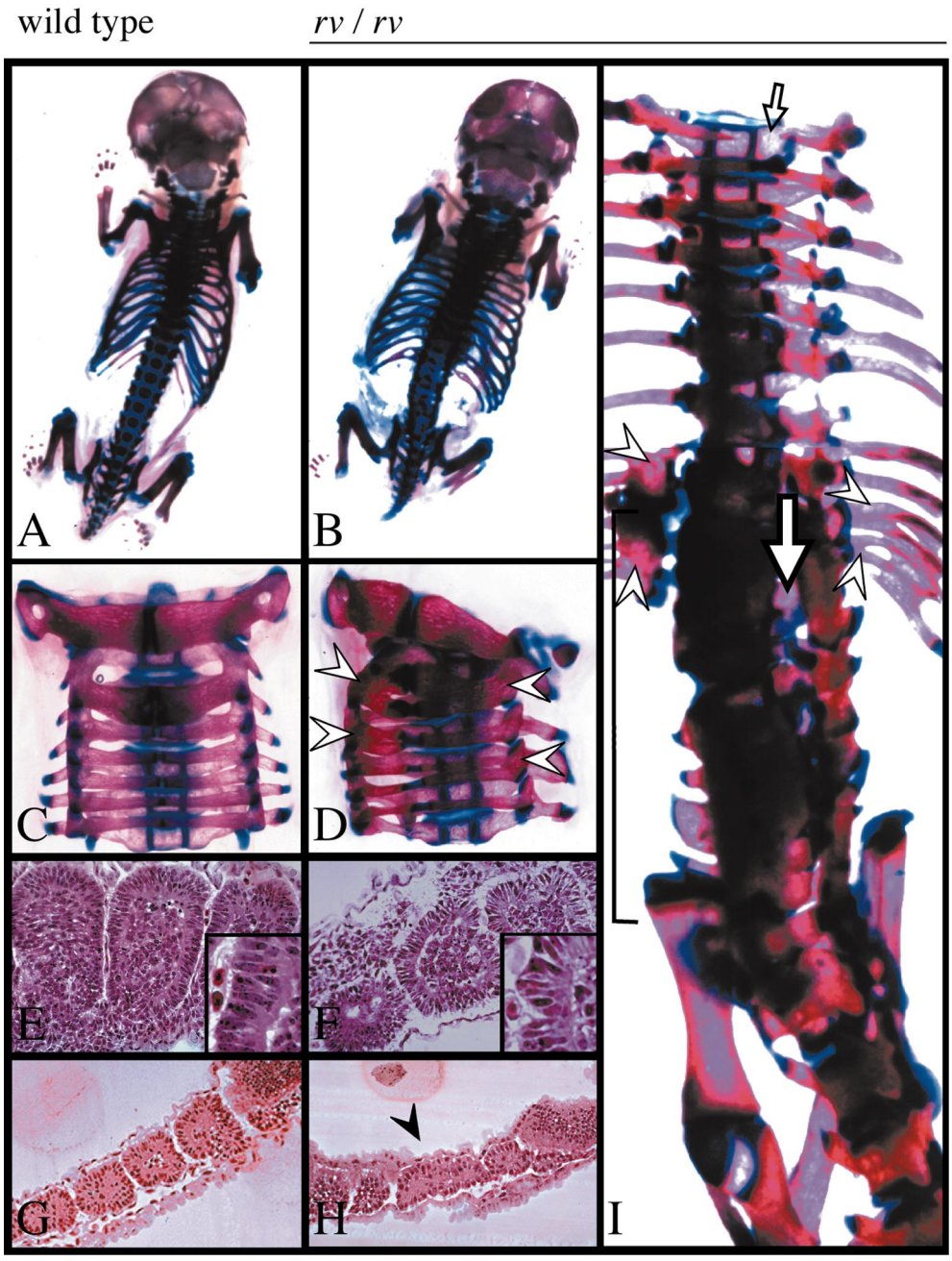

Fig. 1. Vertebral column and somite defects in *rv* mutants. (A,B) skeletal preparations of a wildtype (A) and *rv*/*rv* mutant (B) newborn mouse. In the mutant the vertebral column is characterized by multiple fusions between ribs in the lower thoracic region and fusions of the vertebrae of the cervical, lower thorax, lumbar and sacral regions. The appendicular skeleton and the skull are normal. (C,D) dorsal view of a wildtype (C) and *rv*/*rv* mutant (D) cervical vertebral column. In the mutant multiple neural arches are fused (white arrowheads). (E,F) Sagital sections of day 12.5 wild type (E) and *rv* mutant (F) embryos. In the mutant, the somitic epithelium is disorganized and cells are not in close contact in the baso-lateral regions. (G,H) sagital sections of 7 somites-stage wild type (G) and *rv* mutant (H) embryos. In the mutant, somites are fused (arrowhead) and irregular in shape. (I) Vertebral column of a *rv*/*rv* mutant mouse from the first thoracic vertebra (T 1) to the proximal region of the tail. The neural arches of T 1 are not fused at the dorsal midline (open arrow). The ribs of the lower thorax (T 7 and more caudal) are fused proximally (arrowheads), the vertebral elements of the lower thoracic, lumbar and upper sacral regions are fused to an essentially contiguous bone (bracket), and the neural arches in this region are not fused along the dorsal midline (large arrow).

tion, in serial sections no fully epitheliarized somites were detected more posteriorly in the prospective lumbar region (data not shown).

To characterize the ontogeny of the mutant phenotype and to define the patterning defects in the somites we analyzed the expression of marker genes for various cell populations in the presomitic and somitic mesoderm by whole-mount in situ hybridization. We focused on embryos around day 9.5 of development. At this stage (Theiler Stage (TS) 15) between 21 and 29 somites have been formed, so

that the somites that are just being generated by the presomitic mesoderm are precursors of the lower thoracic or lumbar vertebrae (the region that is severely affected in *rv* homozygotes). The analysis of markers for dermomyotome and sclerotome (*paraxis*, Burgess et al., 1995) myotome (*myogenin*, Montarras et al., 1991) and sclerotome (*Pax9*, Neubüser et al., 1995) showed that the cellular differentiation products of somites were present in mutant embryos and arranged in a largely normal, segmented pattern. However, paraxis expression was significantly reduced (Fig. 2A–D) and *Pax9* expression was diffuse, particularly in the most recently formed somites (Fig. 2E,F), suggesting that sclerotome formation may be impaired. *Myogenin* expression revealed localized perturbations in the arrangement of myotomes such as small partial fusions (open arrow in Fig. 2H), bifurcations (arrowhead in Fig. 2H), and size reductions and gaps (arrows in Fig. 2H). In wild type embryos, *Mox1* has a domain of strong expression in the posterior portion of somites and a weak domain in anterior somite compartments (Fig. 2I; Candia et al., 1992). In

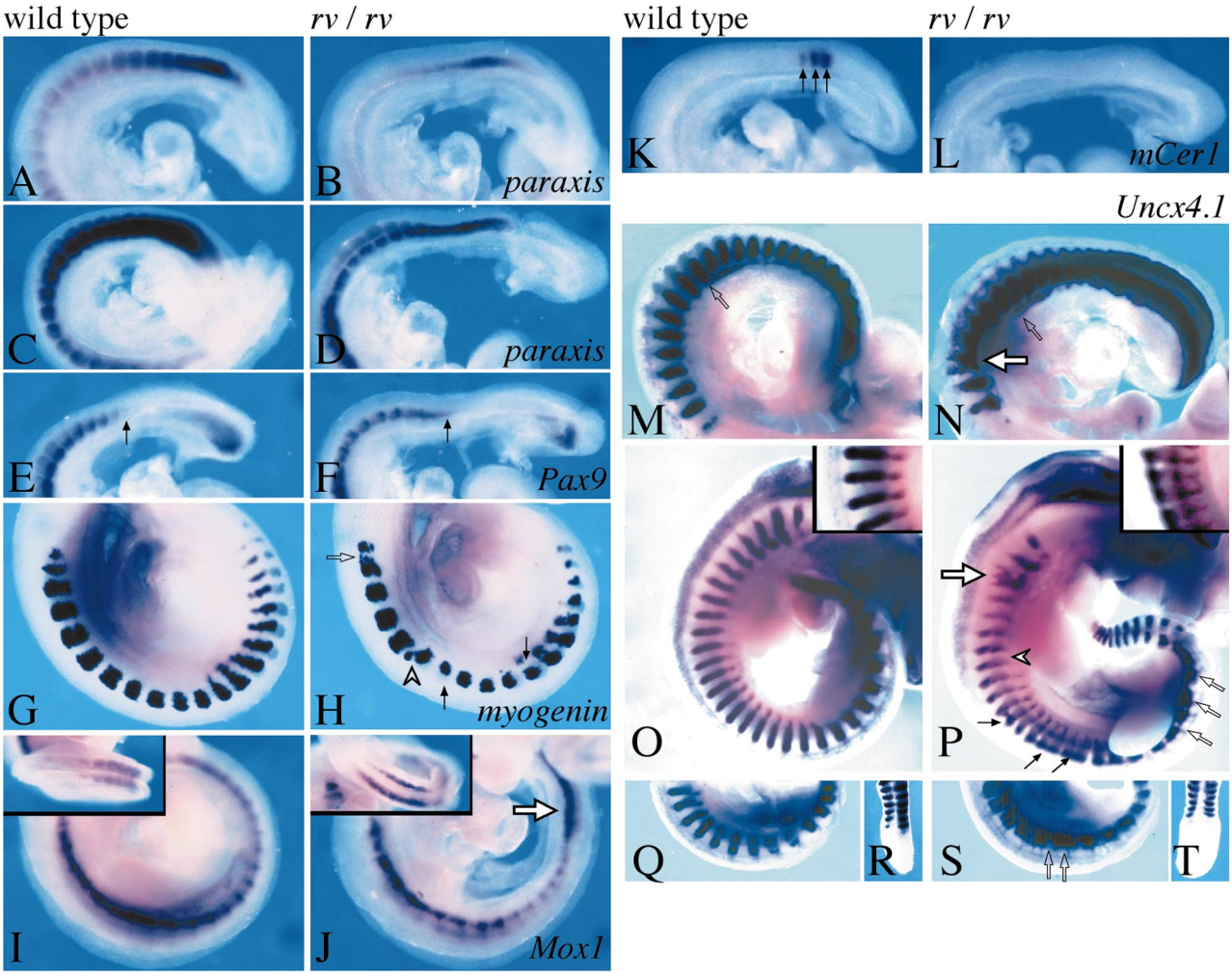

Fig. 2. Defective somite patterning in *rv* mutant embryos. Whole-mount in situ hybridizations of E9.5 (A–N) and E10.5 (O–T) embryos. Short (4 h; A,B) and long (over night; C,D) staining of whole-mount in situ-hybridizations with a *paraxis* probe showing that expression is strongly reduced in *rv*/*rv* embryos. Expression of *Pax9* is diffuse in posterior somites of *rv*/*rv* mutant embryos (F) and the posterior border of expression (arrow) is shifted anteriorly, whereas the segmented expression is evident in the same region of the wild type embryo (E). *Myogenin* expression in *rv*/*rv* mutant embryos (H) indicates myotome defects such as a fusion between adjacent myotomes (open arrow), bifurcations (arrowhead), and gaps or reductions of myotomes (small arrows). *Mox1* expression is reduced in anterior somites of mutants (J) as compared to wildtype embryos (I). In contrast, expression in the most recently formed somites is enhanced (open arrow in J) and the segmented expression is not well defined (compare insets). *mCer1* is expressed in the most recently formed somites, nascent somites and in a stripe in the presomitic mesoderm of wildtype embryos (arrows in K), but *mCer1* transcripts are missing in *rv*/*rv* mutant embryos (L). In day 9.5 *rv*/*rv* embryos anterior (*Uncx4.1* non-expressing) somite compartments are reduced and *Uncx4.1* expression domains fuse (e.g. large arrow in N). Small open arrows in (M,N) point to the anterior end of the (*Uncx4.1* expressing) pronephros. At E10.5 fusions of *Uncx4.1* expression domains are evident in the cervical region (large open arrow in P), the lower thorax (small arrows in P, and inset) and lumbar and sacral region (small open arrows in P and S) of mutant embryos in contrast to wildtype embryos (M,O,Q,R) where *Uncx4.1* expression is strictly segmented. The arrowhead in (P) points to regions of weak ectopic *Uncx4.1* expression in the upper thoracic region. In the tail region of mutant embryos (T) *Uncx4.1* expression appears mostly normal, although the presomitic mesoderm is enlarged in mutants compared to wildtype embryos (R).

mutant embryos, *Mox1* was still differentially expressed in these regions but expression appeared irregular in the cervical region, and expression levels were significantly reduced. In contrast, expression in the most recently formed four to five somites was enhanced and segmented expression was not well defined (arrow and inset in Fig. 2J). The expression of these markers in *rv* mutants indicates that cells of the somitic mesoderm – although irregular in their epithelial organization – differentiate into sclerotomal, dermomyotomal and myotomal populations.

To address whether the polarity of somites might be affected in *rv* mutant embryos we analyzed expression of *mCer1* and *Uncx4.1*. In wild type embryos, *mCer1* is expressed in the anterior portions of the most recently formed and nascent somites, and in a stripe in the anterior presomitic mesoderm (Fig. 2K; Biben et al., 1998; Shawlot et al., 1998; del Barco Barrantes et al., 1999). *Uncx4.1* expression marks the posterior halves of epithelial somites and subsequently the posterior lateral sclerotome (Fig. 2M,O,Q,R; Mansouri et al., 1997; Neidhardt et al., 1997). In *rv* mutant embryos, no *mCer1* expression was detected (Fig. 2L). Conversely, *Uncx4.1* expression domains were expanded and partly fused between segments in day 9.5 embryos (large arrow in Fig. 2N). The (*Uncx4.1* negative) anterior somite compartments were significantly shorter (Fig. 2M,N). Fusions between adjacent *Uncx4.1* expressing regions were consistently found in the cervical (large open arrow Fig. 2P), lower thoracic (small arrows Fig. 2P), and lumbo-sacral (small open arrows Fig. 2P,S) regions. Fusions in the lower thoracic region occurred dorsally and ventrally and were frequently accompanied by regions of reduced expression between such fusions (inset in Fig. 2P). In the sclerotomes of the prospective upper thoracic region, domains of weak expanded *Uncx4.1* expression were found in ventral portions (arrowhead in Fig. 2P). At this stage, expression in the caudal somites appeared normal (Fig. 2T). However, the presomitic mesoderm was enlarged (compare Fig. 2R with Fig. 2T). The regions of clearly disturbed *Uncx4.1* expression in the somites of mutant embryos correspond to the most severely affected portions of the vertebral column. This suggests that the anterior-posterior patterning of somites is altered in the affected regions of *rv* mutants.

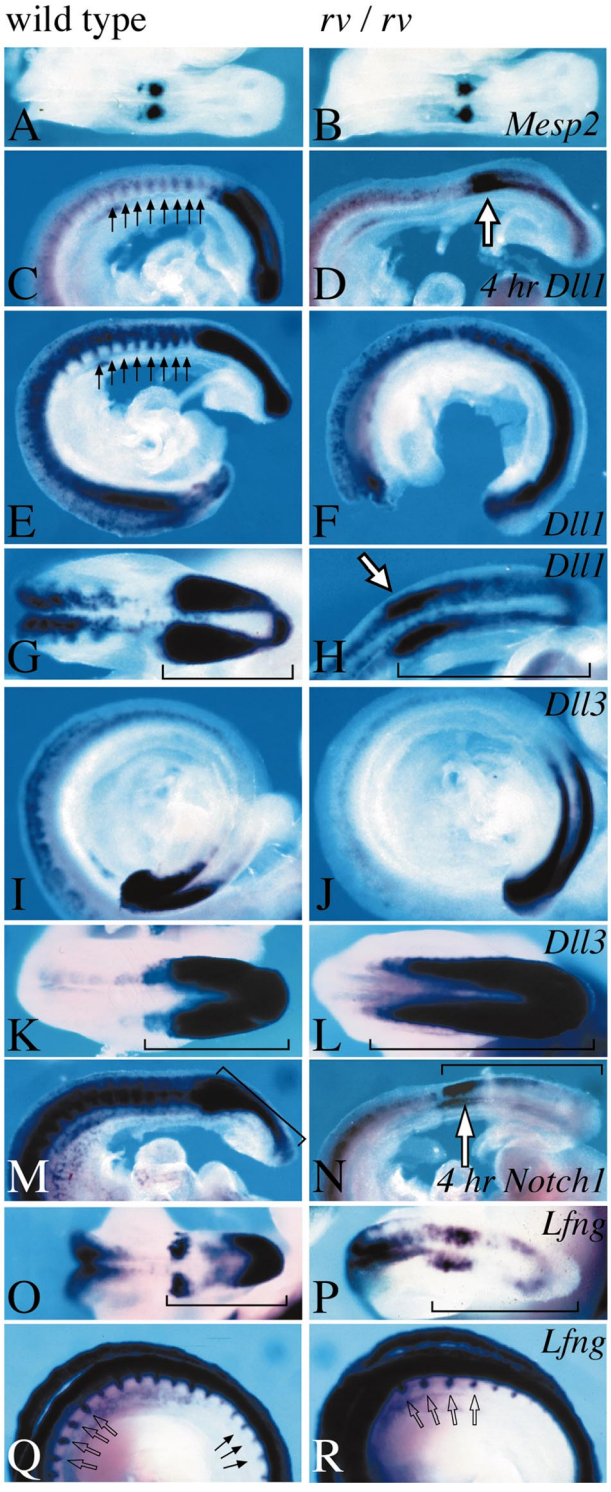

Fig. 3. Altered expression of Notch pathway components in *rv* mutant embryos. Whole-mount in situ-hybridizations of E9.5 wildtype and *rv*/*rv* embryos. Expression of *Mesp2* in the anterior presomitic mesoderm of wildtype (A) and mutant embryos (B) is similar. Expression in the paraxial mesoderm of *Dll1* as detected after 4 h (C,D) or after overnight (E–H) staining is reduced (D,H). In the somites expression in posterior compartments (arrows in C,E) is lost or barely detectable in mutant embryos (D,F). The contiguous *Dll1* expression in the presomitic mesoderm and the region of strongest expression in the anterior presomitic mesoderm (large open arrows in H and D) appear extended and shifted anteriorly in mutant embryos (compare brackets in G and H). Like *Dll1*, expression of *Dll3* is expanded anteriorly in mutant embryos (J,L) compared to wildtype embryos (I, K; compare brackets in K and L). The overall expression of *Notch1* is reduced in *rv*/*rv* embryos (N) compared to wildtype embryos (M). The region of strongest Notch1 expression in the anterior presomitic mesoderm (large open arrow in N) appears to be shifted anteriorly (compare brackets in M and N). Expression of *Lfng* appears essentially normal in the presomitic mesoderm of mutant embryos (P) except that the anterior limit of its expression domain is more anterior (compare brackets in O and P) and levels may be reduced. *Lfng* expression at the posterior somite margins in caudal somites (small arrows in Q) is severely reduced in mutant embryos whereas expression is apparently normal in the rostral region (open arrows in Q and R).

Anterior-posterior somite patterning is also disrupted in *Mesp2* mutants (Saga et al., 1997) as well as in embryos mutant for various Notch pathway components (Conlon et al., 1995; Hrabé de Angelis et al., 1997; Evrard et al., 1998; Kusumi et al., 1998; Zhang and Gridley, 1998). In addition, *rv* genetically interacts with the Delta1 null-allele (*Dll1*^{lacZ}, Hrabé de Angelis et al., 1997). Therefore, we analyzed the expression of *Mesp2* and the Notch pathway components *Dll1*, *Dll3*, Notch1, and *Lfng*. *Mesp2* expression was apparently unaffected in *rv* mutant embryos (Fig. 3B). However, expression of the Notch pathway components was significantly altered. *Dll1* expression in the paraxial mesoderm was generally reduced and expression in the posterior somite compartments was either absent or barely detectable in mutants (Fig. 3D,F). The region of contiguous *Dll1* expression in the presomitic mesoderm (bracket in Fig. 3G) was expanded anteriorly in mutants (Fig. 3H) and *Dll1* expression levels were highest in the anterior-most portion of this expression domain (arrows in Fig. 3D,H). Similarly, the 'presomitic' expression domains of *Dll3*, Notch1 and *Lfng* were expanded anteriorly (Fig. 3J,L,N,P). *Lfng* oscillations in the presomitic mesoderm were apparently normal as indicated by different expression patterns in several homozygous *rv* embryos representing various phases of the described waves of *Lfng* transcription (data not shown), although expression levels might be reduced (Fig. 3P). Like *Dll1*, Notch1 transcripts were clearly less abundant in mutant embryos whereas *Dll3* levels were not obviously altered. *Lfng* transcripts at the posterior somite margins were apparently normal in the cervical region (open arrows Fig. 3R), but reduced or absent posteriorly. Together these results demonstrate that the abundance and distribution of mRNAs encoding specific Notch pathway components are altered in particular regions of *rv* mutant embryos.

2.2. Genetic interaction between rv and the Dll1^{lacZ} loss-of-function allele

The *Dll1*^{lacZ} and the *Dll3*^{pu} alleles genetically interact such that the presence of one copy of the *Dll1*^{lacZ} allele enhances the homozygous *Dll3*^{pu} phenotype and leads to perinatal lethality (J. Beckers and A. Gossler, unpublished observations), suggesting that dosage sensitive genetic interactions could reveal the involvement of other, thus far unknown genes in Notch pathway functions during somito-

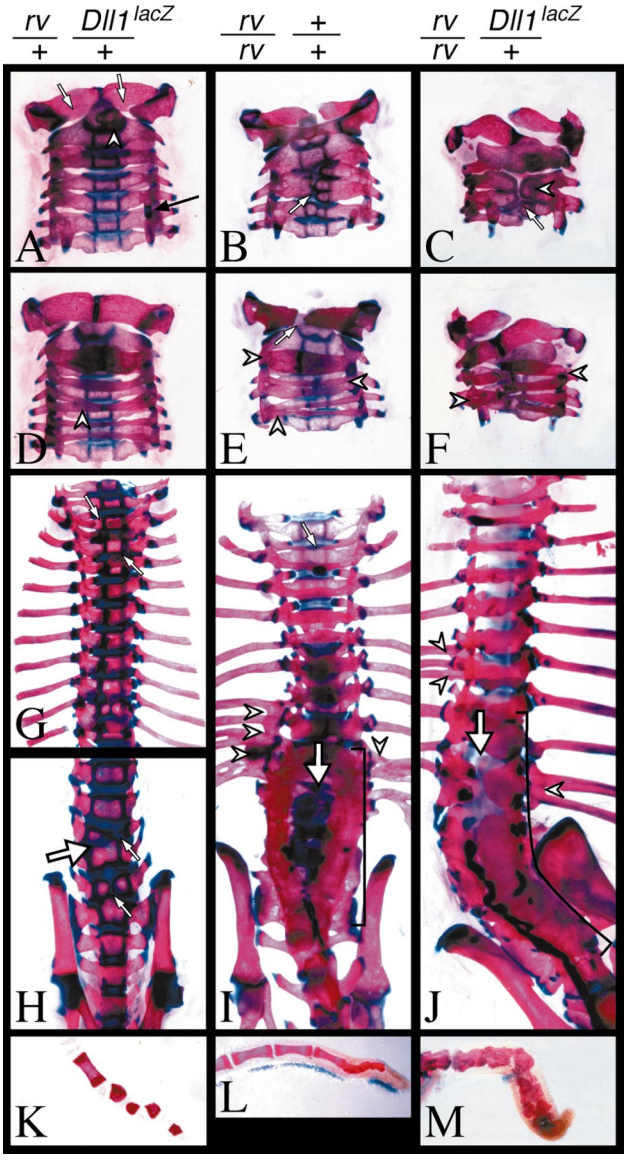

Fig. 4. Skeletal defects in *rv* / *Dll1*^{lacZ} compound mutants. Ventral (A–C) and dorsal (D–F) views of skeletal preparations of cervical vertebral columns. In the double heterozygous mutant a central portion of the ventral arch (arrowhead in A) is not connected to the neural arch (white arrows in A point to gaps between neural and ventral arch), and the neural arches of c4 and c5 are fused (arrowhead in D). Thew ventral process characteristic for c6 is also on c5 (black arrow). In the *rv* homozygous mutant adjacent vertebral bodies are fused and vertebral bodies ventrally split (white arrow in B), neural arches of c2/c3, c4/c5, and c6/7 are fused, respectively (arrowheads in E), and the neural arch of the atlas is split (arrow in E). In the homozygous *rv* mutant which carries one copy of *Dll1*^{lacZ} these defects are more severe and the cervical vertebral column is significantly shorter (C, F). Multiple vertebral bodies are split (arrow in C) or fused (arrowhead in C), and neural arches are fused (arrowheads in F) or partly missing (F) resulting in a severely distorted arrangement of vertebral elements. (G,H) Dorsal (G) and ventral (H) view of the thoracic (G) and lumbosacral (H) region of a double heterozygous mouse; arrows in (G) point to gaps in the laminae of neural arches. In the lumbar region adjacent vertebral bodies are partially fused (large arrow in H) and split (small arrows in H). (I) Dorsal view of the thoracic, lumbar and sacral vertebral column of a homozygous *rv* mouse. A neural arch in the upper thoracic region is split (small arrow), ribs in the lower thoraric region are proximally fused (arrow heads), neural arches are fused from the lower thoracic through the lumbar region including the first or second sacral vertebrae (bracket), and are dorsally split (large arrow). (J) Dorsal view of the thoracic, lumbar and sacral vertebral column of a homozygous *rv* mouse that carries one copy of *Dll1*^{lacZ}. Proximal ribs are fused in the lower thoracic region (arrowheads) and neural arches are dorsally open (large arrow). Fusions of neural arches extend more posteriorly and include the entire sacral region (bracket). Irregular vertebral elements are present in the distal end of the tail in double heterozygous (K) and *rv* homozygous animals (L). In contrast, the tail of a mouse that is homozygous for the *rv* mutation and carries one *Dll1*^{lacZ} allele is reduced to a few irregular vertebral elements (M).

genesis. To test whether *rv* might interact with the Notch pathway, we crossed homozygous *rv* mice to *Dll1*^{lacZ} (Hrabé de Angelis et al., 1997), *Dll3*^{pu} (Kusumi et al., 1998) and *Notch1*^{in32} (Swiatek et al., 1994) mutants, respectively. Mice that are heterozygous for the *rv* mutation have a normal axial skeleton ($n = 4$; data not shown). Likewise, no abnormalities were found in skeletal preparations of double heterozygous *rv*/*Dll3*^{pu} mutants ($n = 5$) or in double heterozygous *rv*/*Notch1*^{in32} ($n = 8$) mice (data not shown). In contrast, mice that were double heterozygous for the *rv* mutation and the *Dll1*^{lacZ} allele had kinked tails (13/16) and were analyzed further.

Skeletal preparations of double heterozygous mutants with and without obvious tail kinks showed that all had vertebral malformations in different regions of the axial skeleton ($n = 6$). All examined mice had irregular vertebral elements in the cervical region (Fig. 4A,D). Fusions occurred between the neural arches ($n = 5$) of cervical vertebra (cv) 4 and cv5, or cv3 and cv4 (arrowhead in Fig. 4D). In some cases the ventral arch of the atlas (cv1) was split ($n = 2$) (open arrows in Fig. 4A) with an isolated ventral remnant (arrow head in Fig. 4A), or the body of the axis (cv2) was irregular ($n = 5$). The ventral process characteristic of cv6 occasionally occurred on cv5 (black arrow in Fig. 4A; $n = 2$) or the neural arch of the axis (cv2) was significantly broadened ($n = 1$). All skeletons of this group had combinations of these irregularities in the cervical region and none of them showed all these characteristics at the same time. In the thoracic, lumbar and sacral regions two double heterozygous animals had no irregularities, in the remaining skeletons vertebral defects were mild and variable. We found fusions between the neural arches of thoracic vertebrae (T) 2 and T3 ($n = 1$) or between T3 and T4 ($n = 2$). In three mice neural arches were not fused in the midline or were partially missing (arrows in Fig. 4G). The ribs appeared always normal in these animals. In the lumbar and sacral regions we found single or multiple irregularly shaped or open neural arches ($n = 2$), split vertebral bodies (small arrow in Fig. 4H) and vertebral bodies with irregular shape or fusions (large arrow in Fig. 4H; $n = 3$). In one case the sixth lumbar vertebra (L6) was fused to the first sacral vertebra (S1). Whereas the phenotypic alterations in the thoracic, lumbar and sacral regions were variable, all double heterozygous animals had – to a varying degree – irregularly shaped vertebral elements in the distal end of the tail (Fig. 4K). Taken together, double heterozygous mutants showed mild vertebral defects in the regions also affected in homozygous *rv* mutants, indicating that the *rv* and *Dll1*^{lacZ} alleles act synergistically.

To address how the *Dll1*^{lacZ} allele affects the phenotype in homozygous *rv* mice, double heterozygous *Dll1*^{lacZ}/*rv* mice were crossed to homozygous *rv* mutants. Offspring were scored for their external phenotype and typed for the presence of the *Dll1*^{lacZ} allele. From a total of 43 offspring from this cross only one mouse with a homozygous *rv* phenotype (confirmed by breeding to homozygous *rv* mutants) that carried the *Dll1*^{lacZ} allele was obtained (Fig. 5). Thus, mice that are homozygous for the *rv*-mutation and heterozygous for the *Dll1*^{lacZ} allele are highly under-represented at birth ($P < 0.01$). The significant deviation from

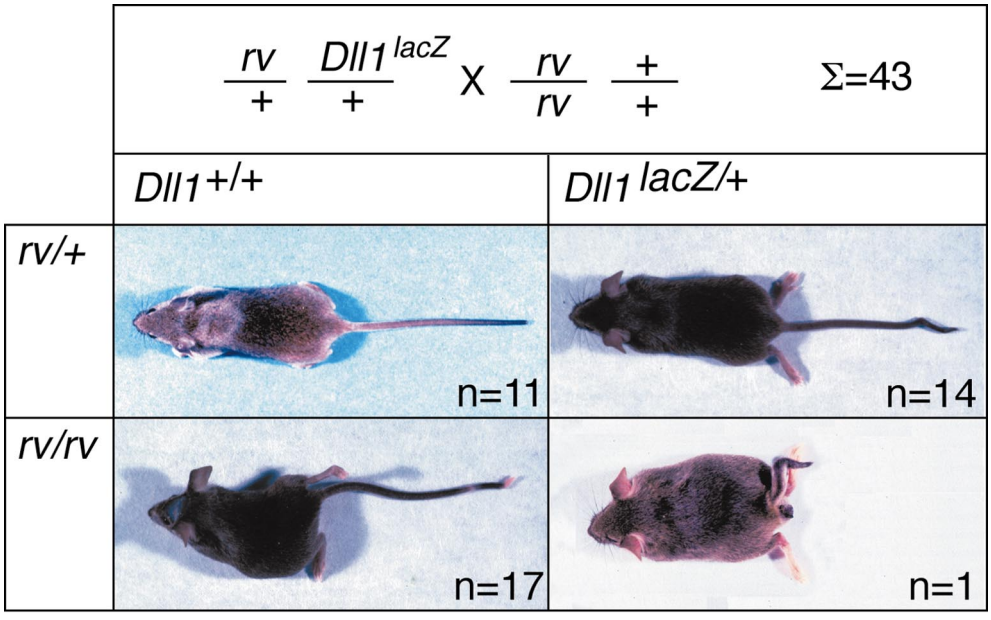

Fig. 5. External phenotype and number of progeny obtained from *rv*/+,Dll1$^{lacZ/+}$ × *rv*/*rv*, + /+ matings. Mice that are heterozygous for the *rv* mutation are externally normal (top left). Mice that are double heterozygous for the *Dll1*^{lacZ} allele and the *rv* mutation have tail kinks in the distal tail region (top right). Externally, mice that are homozygous for *rv* also have a kink in the distal tail and, in addition, frequently have a short body (bottom left). Occasionally, one or both hindlimbs are paralyzed (probably due to compression of spinal nerves caused by vertebral malformations. Mice that are homozygous for the *rv* mutation and in addition heterozygous for the *Dll1*^{lacZ} allele are under-represented at birth and, in contrast to *rv* homozygotes, have a truncated tail (bottom right).

the expected Mendelian Ratio of 25% suggests that the majority of fetuses of this genotype died pre- or perinatally. In contrast to homozygous *rv* mutants, mice with the genotype *rv/rv;Dll1*^{lacZ}/+ ($n = 3$; from this and other crosses) had a severely shortened or truncated tail (Figs. 4M and 5). The cervical vertebral column was shortened and highly disorganized with multiple fused and split neural arches and vertebral bodies (Fig. 4C,F). Like in homozygous *rv* mice the upper thoracic vertebral column was only mildly affected. Fusions of the neural arches began in the lower thoracic region and in contrast to homozygous *rv* mutants included the whole sacral region (bracket in Fig. 4J). Overall, the presence of the *Dll1*^{lacZ} allele enhanced the *rv* phenotype.

2.3. Genetic mapping

As a prerequisite for the identification of the *rv* gene based on its chromosomal location, and to test whether known components of the Notch pathway might qualify as candidates for the gene affected in the *rv* mutation, we determined its chromosomal localization. One interspecific backcross and one intercross including *rv* was generated with *M. musculus castaneus* (CAST/Ei). From both crosses the DNA of homozygous *rv* progeny (as judged by the presence of kinked tails) was analyzed. The initial genome scan with autosome-specific microsatellite markers was done on DNA from 26 intercross progeny and suggested linkage of *rv* with chromosome 7 (data not shown). To verify the localization of *rv* on chromosome 7 and to determine the chromosomal region more precisely, the haplotypes of 12 microsatellite markers along chromosome 7 (see Section 4) were analyzed on DNA from 60 intercross progeny. The results confirmed the initial chromosomal assignment and placed *rv* between *D7Mit253* and *D7Mit166*. Further analysis reduced the critical region to the interval between *D7Mit66* and *D7Mit165*. Subsequently, we analyzed DNA from 283 backcross and 212 intercross progeny representing a total of 707 meioses for recombination between *rv* and *D7Mit66* and *D7Mit165*, respectively. We identified 19 recombinant mice in the backcross and 17 in the intercross. Recombinants were further analyzed with *Mit* markers from the critical region. The locus order and inter-locus distance (in cM ± standard error) for the *rv* gene region deduced from our analysis is *D7Mit66*4.24 ± 1.2 *D7Mit206, 9, 358* 1.06 ± 0.61 *rv, D7Mit164* 0.71 ± 0.5 *D7Mit188* 0.35 ± 0.35 *D7Mit105* 0.35 ± 0.35 *D7Mit165* for the backcross, and *D7Mit66*2.36 ± 0.74 *D7Mit*206, 9, 358 0.23 ± 0.24 *rv, D7Mit188* 0.23 ± 0.24 *D2Mit105* 0.94 ± 0.47 *D7Mit165*for the intercross. None of the genes encoding known components of the Notch pathway except for *RBPjκ* whose chromosomal location is not known (http://www.informatics.jax.org) are contained within the genomic interval that includes the *rv* mutation.

Mesp2 mutants have defects in somite formation and patterning, and the *Mesp2* and *Mesp1* genes map to the vicinity of the *rv* mutation. Despite its apparently normal expression in mutant embryos, we tested whether *Mesp2* is tightly linked and a candidate for the gene affected in the *rv* mutation (a potentially hypomorphic allele). Two out of five analyzed non-recombinants in the *rv*-containing interval between D7Mit253 and D7Mit166 showed recombination between the *rv* mutation and *Mesp2* (data not shown; see Materials and Methods for details), indicating that *Mesp2* is located outside the critical interval. These observations exclude *Mesp2* and *Mesp1* (which resides within 20 kb from *Mesp2*; Saga, 1998) as candidate genes for the *rv* mutation.

3. Discussion

3.1. The developmental origin of vertebral fusions in rv mutants

The segmental defects in the vertebral column of homozygous rib-vertebrae (*rv*) mutants can be traced back to irregularities in size and shape of somites during development (this study and Theiler and Varnum, 1985). Our analysis shows that histopathological defects and irregularities in gene expression are present from early stages of somitogenesis onwards. Theses defects are most evident in those regions of the embryo that correspond to the most severely affected regions of the adult body, i.e. the cervical region and the region from the lower thorax to the upper sacrum. Histopathological defects in *rv* mutant embryos are fusions between somites, disorganization of the somitic epithelium, and incomplete somite epitheliarization. Epitheliarization of somites requires the bHLH protein paraxis (Burgess et al., 1996). Since *paraxis* expression is downregulated in *rv* mutant embryos reduced *paraxis* function may contribute to the disrupted epithelial morphology.

The analysis of molecular markers suggests that the regular anterior-posterior patterning of somites is strongly affected in *rv* mutant embryos, such that anterior compartments are reduced in size or have at least partially acquired characteristics of posterior segment halves. As a consequence, posterior compartments of adjacent somites lie in close proximity and fuse in the most strongly affected regions along the anterior-posterior body axis. The posterior lateral sclerotome cells marked by *Uncx4.1* expression give rise to the pedicles of the vertebrae, most of the laminae of the neural arches, and the proximal ribs (Huang et al., 1994, 1996). Since the confrontation of anterior with posterior somite halves is required to maintain segment borders during differentiation (Stern and Keynes, 1987; Hrabé de Angelis et al., 1997), the fusion of posterior compartments is highly likely to be the earliest manifestation and probably also the cause of the subsequent fusions of proximal ribs, neural arches and vertebral bodies in the cervical, lower thoracic and lumbar regions.

In addition, the transition between the unsegmented

presomitic and the somitic mesoderm in *rv* mutant embryos at E9.5 is indistinct, the presomitic mesoderm appears enlarged (Fig. 3) and *mCer1* expression in the anterior presomitic mesoderm and nascent somites is abolished. This suggests that patterning defects in segmentation may originate already prior to somite formation within the presomitic mesoderm and/or nascent somites.

3.2. The requirement of Delta1 signaling for the compartmentalization of somites

In mice that are deficient for the *Delta1* gene (due to the *Dll1*^{lacZ} loss-of-function allele) the characteristics of posterior segment halves are lost (Hrabé de Angelis et al., 1997). In contrast, the strong reduction or loss of *Delta1* expression in the somites of *rv* mutant embryos is accompanied by size reductions or partial transformations of anterior segment halves into posterior compartments, i.e. posterior segment halves appear to be expanded. The analysis of *Dll1* null mutants indicated that *Delta1* function is required for the generation of posterior segment compartments, but left open whether this function is required in the presomitic mesoderm, or in the somites, or both. In *rv* mutant embryos *Dll1* expression was absent or barely detected in posterior somite halves, but posterior compartments were expanded rather than reduced. This suggests that *Delta1* expression within the segmented mesoderm is not required to confer posterior identities to somite halves, implying that *Delta1* function is critical for establishing and maintaining posterior half-segment identity in either the presomitic mesoderm or the nascent somites (or both) but not in mature somites. Likewise, the loss of *Uncx4.1* expression in *Dll1* mutant embryos (del Barco Barrantes et al., 1999) suggested that *Uncx4.1* could be a target of the *Dll1* signal in the paraxial mesoderm. However, despite the loss or strong reduction of *Dll1* expression in posterior somite halves, *Uncx4.1* is expressed – although in a highly irregular pattern – at apparently normal levels in somites of *rv* mutant embryos. This suggests that the *Dll1* signal in posterior somite halves is not required for *Uncx4.1* expression, or residual *Dll1* expression in somites of *rv* mutants is sufficient to activate or maintain *Uncx4.1*. Alternatively, *Dll1* function in the presomitic mesoderm (where *Dll1* is still expressed in *rv* mutants) could be critical for activation of *Uncx4.1*, and the maintenance *of Uncx4.1* expression does not require *Dll1* in the segmented mesoderm.

3.3. Notch signaling is altered in rv mutant embryos

The phenotype observed in *rv* mutant embryos is reminiscent of mesodermal patterning defects found in mutants carrying loss-of-function alleles of Notch pathway components such as *Dll1*, *Dll3* or *Lfng*. This suggests that *rv* may function in the same patterning process(es) as Notch signaling during somitogenesis. The expression of all analyzed Notch pathway components in the apparently unsegmented paraxial mesoderm was expanded anteriorly at E9.5, suggesting that the 'presomitic' mesoderm may be larger than in wildtype embryos. *Dll1* and *Notch1* mRNA levels were significantly reduced in this region, indicating that the *rv* mutation interferes with the proper expression of these genes. Since the posterior borders of *paraxis* and *Pax9* expression domains also appear to be shifted anteriorly (Fig. 2B,F), the expansion and anterior shift of gene expression domains is likely to be a consequence of morphological alterations, i.e. the expansion of the presomitic mesoderm, rather than a direct consequence of gene regulation. However, since the expression levels of Notch pathway genes were differently affected (*Lfng* or *Dll3* were only mildly affected or indistinguishable from wild type embryos), *rv* might affect *Dll1* and *Notch1*expression specifically. This is further supported by the synergistic genetic interaction between the *rv* mutation and the *Dll1*^{lacZ} allele. Whether the *rv* mutation affects expression of Notch pathway components directly or indirectly, altered Notch signaling is likely to contribute to the somite defects observed in *rv* mutant embryos.

3.4. Genetic interaction between rv and Dll1^{lacZ}

The *rv* mutation and the *Dll1*^{lacZ} loss-of-function allele interact genetically. This interaction is sensitive to gene dosage and leads to vertebral defects in double heterozygotes. Thus, the *Dll1*^{lacZ} allele may be considered an 'enhancer' of the *rv* mutation (and vice versa). The genetic combination of one copy of the *rv* allele and the *Dll1*^{lacZ} (null) allele may reduce *Dll1* levels and thereby lead to disturbed somite patterning and consequently to the relatively mild vertebral defects. This interpretation is consistent with the enhanced phenotype found in homozygous *rv* mice that also carry one copy of the *Dll1*^{lacZ} allele compared to homozygous *rv*mutants and supports the notion that altered Notch signaling might contribute to the *rv* mutant phenotype. Since *Dll1* expression is already significantly reduced in *rv* homozygotes, the addition of one *Dll1*^{lacZ} allele may further reduce *Dll1* levels below the threshold required for somite formation and patterning. This may generate abnormalities that are incompatible with fetal or postnatal survival in the majority of mice. No genetic interaction was detected between *rv* and the *Dll3*^{pu} or *Notch1*^{in32} alleles in double heterozygous mutants. However, whereas *Dll3* levels appear unaffected in *rv* mutants (which might explain the absence of synergistic effects in double heterozygotes) Notch1 levels were strongly reduced similar to *Dll1*. The absence of a phenotype in double heterozygous *rv/Notch1*^{in32} mice may indicate that Notch1 levels are less critical for normal somitogenesis which is consistent with the less severe patterning defects in Notch1 mutants compared to *Dll1* mutants (Swiatek et al., 1994; Conlon et al., 1995; del Barco Barrantes et al., 1999).

Our fine genetic mapping has defined an interval of approximately 1 cM on chromosome 7 containing *rv*. None of the known Notch pathway components in mouse

maps to this genomic region. The chromosomal localization of *RBPjκ* is not known. However, *RBPjκ* is unlikely to be affected in *rv* mutants, since its loss-of-function does not reduce *Dll1* expression in the presomitic mesoderm and leads to up-regulation of *Dll1* expression in the CNS (de la Pompa et al., 1997), which we did not observe in *rv* mutant embryos. Thus, it is unlikely that the *rv* mutation affects a known component of the Notch signaling pathway in mice.

4. Materials and methods

4.1. Histology and skeletal preparation

For histological analysis embryos were embedded in methacrylate (Historesin, Leica) following manufacturers instructions, and sectioned at 4 μm. Slides were stained with eosin/hematoxylin and mounted with permount following standard procedures. Skeleton preparations were done as described by Zachgo et al. (1998).

4.2. Whole-mount in situ-hybridization

Fixation, hybridization, and detection of gene expression in E9.5 and E10.5 embryos was carried out by using standard procedures with probe concentrations between 10 and 50 ng/ml. Bound digoxigenin-11-dUTP labeled riboprobes were detected with alkaline phosphatase conjugated anti-digoxigenin antibodies (Roche). The probes used were *paraxis* (Burgess et al., 1995), *Pax9* (Neubüser et al., 1995), *myogenin* (Montarras et al., 1991), *Mox1* (Candia et al., 1992), *mCer1* (Biben et al., 1998), *Uncx4.1* (Mansouri et al., 1997; Neidhardt et al., 1997), *Mesp2* (Saga et al., 1997), *Dll1* (Bettenhausen et al., 1995), *Dll3* (Kusumi et al., 1998), *Notch1* (Conlon et al., 1995), and *Lfng* (Zhang and Gridley, 1998).

4.3. Chromosomal mapping

Rib-vertebrae (*rv*) arose in C57BL/6 mice, was subsequently maintained on the C57BL/6J background (Theiler and Varnum, 1985) and transferred on a mixed 129/C57 genetic background. Interspecific backcross and intercross animals were generated by mating rv/rv with (rv/rv × Cast/Ei)F1 and (rv/rv × Cast/Ei)F1 with (rv/rv × Cast/Ei)F1 animals, respectively. DNA used for genetic mapping analysis was prepared from spleen or tail biopsy samples, and microsatellite markers (Dietrich et al., 1992) were analyzed by PCR essentially as described by Pavlova et al. (1998). Twenty-six intercross progeny were used to map *rv* to chromosome 7. Chromosome 7 markers used for fine genetic mapping were (in proximal-distal order): *D7MIT323, D7MIT97, D7MIT99, D7MIT66, D7MIT206, D7MIT9, D7MIT358, D7MIT164, D7MIT188, D7MIT105, D7MIT165, D7MIT107, D7MIT187, D7MIT371, D7MIT151, D7MIT207, D7MIT304,* and *D7MIT166*. Additional markers that were tested but were not polymorphic or gave ambiguous results were *D7MIT266, D7MIT224, D7MIT160, D7MIT163, D7MIT237, D7MIT7, D7MIT285, D7MIT67, D7MIT103, D7MIT43, D7MIT134, D7MIT136, D7MIT241, D7MIT208, D7MIT287, D7MIT332,* and *D7MIT360*. Recombination distances were determined with Map Manager v.2.6 (Manly, 1993). Mapping of *Mesp2* was done by Southern blot hybridizations of HindIII digested genomic DNA using a 900 bp *Xba*I fragment of the cDNA as probe, which detects an approximately 15 kb fragment in *M. musculus musculus* DNA, and an additional approximately 9 kb fragment in *M. musculus castaneu*s DNA.

Acknowledgements

We would like to thank our colleagues in the laboratory for discussions and sharing reagents. J.B. was supported by a postdoctoral fellowship from the Deutsche Forschungsgemeinschaft (DFG). This work was facilitated by the core facility of The Jackson Laboratory Cancer Center (CA34196).

References

Artavanis-Tsakonas, S., Matsuno, K., Fortini, M.E., 1995. Notch signaling. Science 268, 225–232.

Artavanis-Tsakonas, S., Rand, M.D., Lake, R.J., 1999. Notch signaling: cell fate control and signal integration in development. Science 284, 770–776.

Bellairs, R., 1963. The development of somites in the chick embryo. J. Embryol. Exp. Morphol. 11, 697–714.

Bettenhausen, B., de Angelis, M.H., Simon, D., Guenet, J.L., Gossler, A., 1995. Transient and restricted expression during mouse embryogenesis of Dll1, a murine gene closely related to Drosophila Delta. Development 121, 2407–2418.

Biben, C., Stanley, E., Fabri, L., Kotecha, S., Rhinn, M., Drinkwater, C., Lah, M., Wang, C.-C., Nash, A., Hilton, D., Ang, S.-L., Mohun, T., Harvey, R.P., 1998. Murine cerberus homologue mCer-1: a candidate anterior patterning molecule. Dev. Biol. 194, 135–151.

Brand, M., Campos-Ortega, J.A., 1990. Second-site modifiers of the split mutation of Notch define genes involved in neurogenesis in Drosophila melanogaster. Roux's Arch. Dev. Biol. 198, 275–285.

Bronner-Fraser, M., Stern, C., 1991. Effects of mesodermal tissues on avian neural crest cell migration. Dev. Biol. 143, 213–217.

Brustis, J., Gipoulou, J., 1973. Potentialites d'organisation et de differenciation du mesoderm somitique non segmente associe aux tissus axiaux (corde dorsale et tube nerveux) chez les amphibiens anoures. C. R. Hebd. Seances Acad. Sci. 276, 85–88.

Burgess, R., Cserjesi, P., Ligon, K.L., Olson, E.N., 1995. Paraxis: a basic helix-loop-helix protein expressed in paraxial mesoderm and developing somites. Dev. Biol. 168, 296–306.

Burgess, R., Rawls, A., Brown, D., Bradley, A., Olson, E., 1996. Requirement of the *paraxis* gene for somite formation and muscoskeletal patterning. Nature 384, 570–573.

Campos-Ortega, J.A., 1995. Genetic mechanisms of early neurogenesis in Drosophila melanogaster. Mol. Neurobiol. 10, 75–89.

Candia, A.F., Hu, J., Crosby, J., Lalley, P.A., Noden, D., Nadeau, J.H., Wright, C.V., 1992. *Mox-1* and *Mox-2* define a novel homeobox gene subfamily and are differentially expressed during early mesodermal patterning in mouse embryos. Development 116, 1123–1136.

Christ, B., Ordahl, C.P., 1995. Early stages of chick somite development. Anat. Embryol. Berl. 191, 381–396.

Christ, B., Jacob, H.J., Jacob, M., 1972. Experimental analysis of somitogenesis in the chick embryo. Z. Anat. Entwicklungsgesch. 138, 82–97.

Christ, B., Jacob, H.J., Jacob, M., 1974. Somitogenesis in the chick embryo. Determination of the segmentation direction. Verh. Anat. Ges. 68, 573–579.

Conlon, R.A., Reaume, A.G., Rossant, J., 1995. *Notch1* is required for the coordinate segmentation of somites. Development 121, 1533–1545.

de Celis, J.F., Garcia Bellido, A., Bray, S.J., 1996. Activation and function of Notch at the dorsal-ventral boundary of the wing imaginal disc. Development 122, 359–369.

de la Pompa, J.L., Wakeham, A., Correia, K.M., Samper, E., Brown, S., Aguilera, R.J., Nakano, T., Honjo, T., Mak, T.W., Rossant, J., Conlon, R.A., 1997. Conservation of the Notch signalling pathway in mammalian neurogenesis. Development 124, 1139–1148.

del Barco Barrantes, I., Elia, A.J., Wünsch, K., Hrabe De Angelis, M., Mak, T.W., Rossant, R., Conlon, R.A., Gossler, A., de la Pompa, J.-L, 1999. Interaction between L-fringe and Notch signalling in the regulation of boundary formation and posterior identity in the presomitic mesoderm of the mouse. Curr. Biol. 9, 470–480.

Dietrich, W., Katz, H., Lincoln, S.E., Shin, H.S., Friedman, J., Dracopoli, N.C., Lander, E.S., 1992. A genetic map of the mouse suitable for typing intraspecific crosses. Genetics 131, 423–447.

Doherty, D., Feger, G., Younger-Shepherd, S., Jan, L.Y., Jan, Y.N., 1996. Delta is a ventral to dorsal signal complementary to Serrate, another Notch ligand, in *Drosophila* wing formation. Genes Dev. 10, 421–434.

Dunwoodie, S.L., Henrique, D., Harrison, S.M., Beddington, R.S., 1997. Mouse Dll3: a novel divergent Delta gene which may complement the function of other Delta homologues during early pattern formation in the mouse embryo. Development 124, 3065–3076.

Evrard, Y.A., Lun, Y., Aulehla, A., Gan, L., Johnson, R.L., 1998. *lunatic fringe* is an essential mediator of somite segmentation and patterning. Nature 394, 377–381.

Forsberg, H., Crozet, F., Brown, N.A., 1998. Waves of mouse Lunatic fringe expression, in four-hour cycles at two-hour intervals, precede somite boundary formation. Curr. Biol. 8, 1027–1030.

Gossler, A., Hrabe de Angelis, M., 1997. Somitogenesis. Curr. Top. Dev. Biol. 38, 225–287.

Hartenstein, A.Y., Rugendorff, A., Tepass, U., Hartenstein, V., 1992. The function of the neurogenic genes during epithelial development in the Drosophila embryo. Development 116, 1203–1220.

Hrabé de Angelis, M., McIntyre II, J., Gossler, A., 1997. Maintenance of somite borders in mice requires the *Delta* homologue *Dll1*. Nature 386, 717–721.

Huang, R., Zhi, Q., Wilting, J., Christ, B., 1994. The fate of somitocoele cells in avian embryos. Anat. Embryol. Berl. 190, 243–250.

Huang, R., Zhi, Q., Neubüser, A., Müller, T.S., Brand-Saberi, B., Christ, B., Wilting, J., 1996. Function of somite and somitocoel cells in the formation of the vertebral motion segment in avian embryos. Acta Anat. 155, 231–241.

Jen, W.C., Wettstein, D., Turner, D., Chitnis, A., Kintner, C., 1997. The Notch ligand X-Delta-2, mediates segmentation of the paraxial mesoderm in *Xenopus* embryos. Development 124, 1169–1178.

Jen, W., Gawantka, V., Pollet, N., Niehrs, C., Kintner, C., 1999. Periodic repression of notch pathway genes governs the segmentation of xenopus embryos. Genes Dev. 13, 1486–1499.

Johnston, S.H., Rauskolb, C., Wilson, R., Prabhakaran, B., Irvine, K.D., Vogt, T.F., 1997. A family of mammalian Fringe genes implicated in boundary determination and the Notch pathway. Development 124, 2245–2254.

Keynes, R.J., Stern, C.D., 1984. Segmentation in the vertebrate nervous system. Nature 310, 786–789.

Keynes, R.J., Stern, C.D., 1988. Mechanisms of vertebrate segmentation. Development 103, 413–429.

Kieny, M., Mauger, A., Sengel, P., 1972. Early regionalization of the somite mesoderm as studied by the development of the axial skeleton of the chick embryo. Dev. Biol. 28, 142–161.

Kusumi, K., Sun, E.S., Kerrebrock, A.W., Bronson, R.T., Chi, D.-C., Bulotsky, M.S., Spencer, J.B., Birren, B.W., Frankel, W.N., Lander, E.S., 1998. The mouse pudgy mutation disrupts *Delta* homologue *Dll3* and initiation of early somite boundaries. Nat. Genet. 19, 274–278.

Lanot, R., 1971. La formation de somites chez l'embryon d'oiseau: etude experimentale. J. Embryol. Exp. Morphol. 26, 1–20.

Manly, K.F., 1993. A Macintosh program for storage and analysis of experimental genetic mapping data. Mamm. Genome 4, 303–313.

Mansouri, A., Yokota, Y., Wehr, R., Copeland, N.G., Jenkins, N.A., Gruss, P., 1997. Paired-related murine homeobox gene expressed in the developing sclerotome, kidney, and nervous system. Dev. Dyn. 210, 53–65.

McGrew, M.J., Dale, J.K., Fraboulet, S., Pourquie, O., 1998. The lunatic Fringe gene is a target of the molecular clock linked to somite segmentation in avian embryos. Curr. Biol. 8, 979–982.

Menkes, B., Sandor, S., 1977. Somitogenesis: regulation potencies, sequence determination and primordial interactions. In: Ede, D.A., Hinchliffe, J.R., Balls, M. (Eds.). Vertebrate Limb and Somite Morphogenesis, Cambridge University Press, Cambridge, pp. 405–419.

Montarras, D., Chelly, J., Bober, E., Arnold, H., Ott, M.-O., Gros, F., Pinset, C., 1991. Developmental patterns in the expression of *Myf5 MyoD*, myogenin, and *MRF4* during myogenesis. New Biol. 3, 592–600.

Neidhardt, L.M., Kispert, A., Herrmann, B.G., 1997. A mouse gene of the paired-related homeobox class expressed in the caudal somite compartment and in the developing vertebral column, kidney and nervous system. Dev. Genes Evol. 207, 330–339.

Neubüser, A., Koseki, H., Balling, R., 1995. Characterization and developmental expression of *Pax9*, a paired-box-containing gene related to *Pax1*. Dev. Biol. 170, 701–716.

Norris, W.E., Stern, C.D., Keynes, R.J., 1989. Molecular differences between the rostral and caudal halves of the sclerotome in the chick embryo. Development 105, 541–548.

Packard Jr., D.S., Jacobson, A.G., 1976. The influence of axial structures on chick somite formation. Dev. Biol. 53, 36–48.

Packard Jr., D.S., 1980a. Somite formation in cultured embryos of the snapping turtle *Chelydra serpentina*. J. Embryol. Exp. Morphol. 59, 113–130.

Packard Jr., D.S., 1980b. Somitogenesis in cultured embryos of the Japanese quail Coturnix coturnix japonica. Am. J. Anat. 158, 83–91.

Palmeirim, I., Henrique, D., Ish-Horowicz, D., Pourquie, O., 1997. Avian hairy gene expression identifies a molecular clock linked to vertebrate segmentation and somitogenesis. Cell 91, 639–648.

Pavlova, M.N., Clark, A.M., Gossler, A., 1998. High-resolution mapping of the truncate (tc) locus on mouse Chromosome 6. Mamm. Genome 9, 843–845.

Qi, H., Rand, M.D., Wu, X., Sestan, N., Wang, W., Rakic, P., Xu, T., Artavanis-Tsakonas, S., 1999. Processing of the Notch ligand Delta by the metalloprotease kuzbanian. Science 283, 91–94.

Saga, Y., 1998. Genetic rescue of segmentation defect in MesP2-deficient mice by MesP1 gene replacement. Mech. Dev. 75, 53–66.

Saga, Y., Hata, N., Koseki, H., Taketo, M.M., 1997. *Mesp2*: a novel mouse gene expressed in the presegmented mesoderm and essential for segmentation initiation. Genes Dev. 11, 1827–1839.

Sandor, S., Fazakas-Todea, I., 1980. Researches on the formation of axial organs in the chick embryo. X. Further investigations on the role of ecto- and endoderm in somitogenesis. Morphol. Embryol. Bucur. 26, 29–32.

Shawlot, W., Deng, J.M., Behringer, R.R., 1998. Expression of the mouse cerberus-related gene Cerr1, suggests a role in anterior neural induction and somitogenesis. Proc. Natl. Acad. Sci. USA 95, 6198–6203.

Sosic, D., Brand-Saberi, B., Schmidt, C., Christ, B., Olson, E.N., 1997. Regulation of *paraxis* expression and somite formation by ectoderm- and neural tube-derived signals. Dev. Biol. 185, 229–243.

Sparrow, D.B., Jen, W.C., Kotecha, S., Towers, N., Kintner, C., Mohun, T.J., 1998. Thylacine 1 is expressed segmentally within the paraxial mesoderm

of the Xenopus embryo and interacts with the Notch pathway. Development 125, 2041–2051.

Stern, C.D., Keynes, R.J., 1987. Interactions between somite cells: the formation and maintenance of segment boundaries in the chick embryo. Development 99, 261–272.

Sundaram, M., Greenwald, I., 1993. Suppressors of a lin-12 hypomorph define genes that interact with both lin-12 and glp-1 in Caenorhabditis elegans. Genetics 135, 765–783.

Swiatek, P.J., Lindsell, C.E., Franco Del Amo, F., Weinmaster, G., Gridley, T., 1994. *Notch1* is essential for postimplantation development in mice. Genes Dev. 8, 707–719.

Takke, C., Campos-Ortega, J.A., 1999. her1, a zebrafish pair-rule like gene, acts downstream of notch signalling to control somite development. Development 126, 3005–3014.

Tam, P.P.L., Beddington, R.S.P., 1986. The metameric organization of the presomitic mesoderm and somite specification in the mouse embryo. In: Bellairs, R. (Ed.). Somites in Developing Embryos, Advanced Science Institutes Series Vol. Life Sciences 118, Plenum Press, New York, pp. 17–36.

Teillet, M.A., Kalcheim, C., Le Douarin, N.M., 1987. Formation of the dorsal root ganglia in the avian embryo: segmental origin and migratory behavior of neural crest progenitor cells. Dev. Biol. 120, 329–347.

Tepass, U., Hartenstein, V., 1995. Neurogenic and proneural genes control cell fate specification in the Drosophila endoderm. Development 121, 393–405.

Theiler, K., Varnum, D.S., 1985. Development of rib-vertebrae: a new mutation in the house mouse with accessory caudal duplications. Anat. Embryol. Berl. 173, 111–116.

Williams, R., Lendahl, U., Lardelli, M., 1995. Complementary and combinatorial patterns of Notch gene family expression during early mouse development. Mech. Dev. 53, 357–368.

Xu, T., Rebay, I., Fleming, R.J., Scottgale, T.N., Artavanis-Tsakonas, S., 1990. The Notch locus and the genetic circuitry involved in early Drosophila neurogenesis. Genes Dev. 4, 464–475.

Zachgo, J., Korn, R., Gossler, A., 1998. Genetic interactions suggest that Danforth's short tail (*Sd*) is a gain-of-function mutation. Dev. Genet. 23, 86–96.

Zhang, N., Gridley, T., 1998. Defects in somite formation in lunatic fringe-deficient mice. Nature 394, 374–377.